AD-A276 497

# New and Emerging Techniques for Imaging Surfaces

DTIC
ELECTE
MAR 0 8 1994
S F D

*Ellen D. Williams*
Department of Physics
University of Maryland
College Park, MD 20742-4111 U.S.A.

and

*L.D. Marks*
Department of Materials Science and Engineering
Northwestern University
Evanston, IL 60208 U.S.A.

## Abstract

The development of techniques for real-time in-situ imaging of surfaces and for spatially resolved spectroscopic imaging of surfaces is reviewed. The capabilities of Field-Ion Microscopy, In-Situ Transmission Electron Microscopy, Low-Energy Electron Microscopy, Point Projection Microscopy, In-Situ Scanning Electron Microscopy, Near-Field Scanning Optical Microscopy, Photo-emission electron microscopy, Plane-view Transmission Electron Microscopy, Reflection Electron Microscopy, Scanning Electron Microscopy with Polarization Analysis, Scanning Micro-cathodoluminescence, and Scanning Tunneling Microscopy are summarized.

This document has been approved for public release and sale; its distribution is unlimited.

Submitted to: Critical Reviews of Surface Chemistry, 1/94

94-06877

94 3 02 022

# NORTHWESTERN UNIVERSITY

ROBERT R. McCORMICK SCHOOL OF
ENGINEERING AND APPLIED SCIENCE

Department of Materials Science and Engineering

Accesion For
NTIS CRA&I ☑
DTIC TAB ☐
Unannounced ☐
Justification
By
Distribution/
Availability Codes
Dist | Avail and/or Special
A-1

February 16, 1994

Scientific Officer Code: 1114SS
Dr. Max N. Yoder
Office of Naval Research
800 N. Quincy Street
Arlington, Virginia 22217-5000

Re: Grant #N00014-93-1-0363
R&T Project Code: 414500lmmy01
"New & Emerging Techniques for Imaging Surfaces Workshop"

Dear Dr. Yoder:

Enclosed are 3 copies of our Final Technical Report for the above grant. I appreciate the continued support from the National Science Foundation.

Very truly yours,

Laurence D. Marks
Professor

cc: Grant Administrator
Office of Naval Research
Resident Representative N62880
536 S. Clark Street
Chicago, IL 60605-1588

Defense Technical Information Center
Building 5, Cameron Station
Alexandria, Virginia 22314

ORSP Office

## I. Overview

The Workshop on New and Emerging Techniques for Imaging Surfaces was organized to bring together scientists working in the forefront of imaging technologies, to allow exchange of information, to compare the capabilities of existing technologies, and to assess the most promising directions of future research. In organizing the conference, a specific decision was made to limit the scope of the conference to imaging, as opposed to diffraction analysis (LEED, RHEED, photo-emission holography). This decision was made to keep a very tight focus to the conference, and in no way reflects a lack of appreciation of the very important advances that are being made in surface crystallography.

The conference was held in April of 1993. Thirty-eight scientists attended the workshop, of whom fourteen were invited speakers (Table I). The invited speakers were requested to provide detailed written technical information about the microscopic techniques which they presented. This information was collated and served as the basis for a discussion held on the last day of the conference, in which the attendees considered the most important new opportunities presented by the recent developments in microscopy. The conclusions of that discussion are summarized in the following sections, and in tables II-IV.

## II. New Opportunities in Microscopy

While a wide range of different techniques was presented, two over-riding themes in the new developments were apparent. These were 1) The development of capabilities for real-time in situ measurements, and 2) The development of capabilities for correlating "spectroscopic" properties with structural properties with nanometer (or better) resolution. Many of the techniques discussed can be used in either of these two modes. However, at present, there is a trade-off between the two capabilities: one generally obtains additional spectroscopic information only by sacrificing acquisition rate or resolution. Increasing the signal-to-noise of the different techniques to allow both types of capabilities to be realized simultaneously will remain one of the technical challenges of future work on instrumentation. However, the present level of capabilities already allow unprecedented opportunities for investigations of surface properties, with the potential for qualitative advances in our ability to understand and control surface processes.

## II.a Real-Time, In-Situ Measurements

Control of any surface modification technique requires understanding the kinetics of the process. This has remained one of the outstanding challenges in Surface Science, because virtually all measurements possible to date have probed some indirect and average result of the kinetics. Because the data thus obtained is influenced by many individual kinetic steps, deducing the important governing mechanisms and rates can only be accomplished by making generally unrealistic simplifying assumptions. Until very recently, the one exception to this rule has been Field Ion Microscopy (FIM), which, as illustrated in Fig. 1, has the capability of measuring kinetic processes, in a snap-shot mode, with atomic resolution [1-5]. The formalism of this type of measurement allows one to begin with the simplicity of individual atomic events, and to use those to construct the complexity of real systems. With the advent of more general real-time imaging capabilities, the philosophy developed in FIM is now realistically available to a wide variety of materials and processing conditions. The importance of applying such measurements in real time under real processing conditions has been demonstrated, for instance, by the powerful diagnostic capabilities of RHEED during MBE growth [6-8]. Recent advances in UHV-TEM have demonstrated the possibility of dynamic high-temperature studies of surfaces viewed in cross section [9,10].

Real-time, *in-situ* measurements require both the capability for rapid imaging, and the means for introducing sample processing conditions simultaneously with the measurement. The speed of imaging is generally limited either by signal-to-noise, or by data acquisition capabilities. Including the capability for *in-situ* sample processing generally places constraints on the mechanical design of the instrument, which may in turn introduce trade-offs in the resolution or speed of the measurement. In general, we may comment that the electron beam methods (Reflection Electron Microscopy (REM), Scanning Reflection Electron Microscopy (SREM) and Low-Energy Electron Microscopy (LEEM)) facilitate high imaging speeds (real time) and high sample temperatures, whereas the Scanning Tunneling Microscope (STM) avoids the geometric distortions of the reflection methods while providing higher resolution. Rapid advances in high temperature and higher speed STM are anticipated. The UHV Plane-View Transmission Electron Microscopy (Plane-view TEM) work is a special case (see below) which avoids geometric distortion. The LEEM and Photoelectron Emission Microscopy (PEEM) techniques also avoid geometric image distortion, but are limited in resolution. Interestingly, the fastest measurements achieved with the electron beam techniques have

been limited not only by the signal-to-noise of microscope, but also by the data acquisition technology, to video rates of 30 frames per second.

REM, LEEM and Plane-view TEM

All three of these techniques are based on the electron scattering mechanisms and electron focusing techniques of standard electron microscopies. Each achieves surface sensitivity in a different way. In REM, the incident electron beam is directed onto the sample at grazing incidence at an energy of ≥ 100 keV [11,12]. This results in good spatial resolution (≈10 vμ at video rates, 1 nm in static mode) in the direction perpendicular to the beam. REM imaging of real time processes, illustrated in Fig. 2, has been demonstrated for growth, for electromigration and for thermally induced structural changes on surfaces at temperatures as high as 1200°C [13-16]. In LEEM [17-20], the sample serves as an element in a retarding immersion lens, allowing the incident beam to be slowed to surface sensitive LEED energies (≈5-200 eV) for normal incidence on the sample. The back-scattered electrons are then reaccelerated through the immersion lens for focusing in the image arm of the microscope. Spatial resolution below 20 nm has been demonstrated. Real-time imaging has been demonstrated for thermally activated processes up to 1200°C [21-23], including changes in surface morphology, as shown in Fig. 3 [24], and evolution of structure during epitaxial growth via metal deposition [23,25-28] as shown in Fig. 4. Spectroscopic variations of LEEM allowing spatially resolved compositional information (Auger Electron Emission Microscopy) and magnetic information (Spin-Polarized Electron Microscopy) are possible with corresponding loss of speed [20,29]. In Plane-view TEM, the electron beam is directed through a thinned sample, providing information about the top and bottom surfaces. Surface sensitivity is obtained either through intensity variation due to differences in sample thickness, phase contrast involving surface diffraction processes or by imaging from bulk-forbidden beams. Imaging has been demonstrated with better than 2 nm lateral sensitivity, and improvements to the atomic scale are predicted [30-32]. Imaging under processing conditions of high temperature and gas-etching have been demonstrated [33], as well as during *in-situ* growth [34,35]. It is also possible to correlate bulk structure, such as grain boundaries and inclusions, with surface structure [36].

Photo-electron Emission Microscopy (PEEM) [37-43]

The contrast mechanisms in photo-electron emission microscopy are the differential probability of excitation of photo-electrons due to variations in work

function or in composition across the surface. PEEM thus uses an incident photon beam of energy greater than about 5 eV to photo-excite electrons. To obtain imaging, the sample is configured as an element in an immersion lens, as in LEEM, so that the emitted photoelectrons can be collected and focused onto a detector. Imaging in PEEM involves a trade-off between speed and resolution. The energy spread of photo-electrons degrades the resolution, so that resolution of only about 200 nm has been observed when there is no energy selection in the imaging optics. However, in this mode there is sufficient signal, even using a laboratory-based UV source, to allow video-rate data acquisition. The application of this technique to chemical adsorption has resulted in significant advances in understanding the kinetics of chemical reaction processes as illustrated in Fig. 5 [44]. Addition of an energy analyzer allows improvements of spatial resolution at the cost of signal-to-noise and thus the rate of data acquisition. This aspect of PEEM is discussed under the heading "Spatially Resolved Spectroscopy".

Scanning Tunneling Microscopy (STM) [45-48]

In scanning tunneling microscopy, "an atomically sharp metal tip is employed as a local probe which is scanned approximately 0.5 nm above the surface. The tip either collects or emits tunneling electrons ( $\leq$1 eV) through the vacuum tunneling barrier between the tip and the sample. The tunneling current is fed directly into a preamplifier, whose output is connected to feedback electronics that set the tunneling current to a target value (typically about 0.1 nA) by controlling the tip-sample separation with a piezo-actuator. The image is formed in a number of ways, *e.g.* by mapping the feedback error signal, tunneling current, differential conductivity of the tunneling gap, etc. as a function of the scanning position of the probe. Both topological and electronic features on the surface give rise to the image contrast. In the most common mode of operation, the constant current mode, the image is a real-space contour of a constant electronic local density of states (LDOS) at the energy set by the tip-sample bias voltage. Imaging by STM is usually non-destructive, although some molecularly bonded surfaces or adsorbates may be sensitive to the tunneling current. It is also possible to create/repair a surface vacancy or to move atoms with the probe tip. The sample environment is quite variable (unlike the true microscopies discussed above): it is possible to image in air, in UHV or in a liquid, and at temperatures ranging from 4K to 1300K."

"Lateral resolution of less than 0.3 nm, and vertical resolution of less than 0.01Å are attainable. The sources of the limitations on resolution in STM include first of all,

the fundamental limit which is set by the spatial extent of the electronic wave function in the vacuum region near the tip apex. This depends on both the structure and chemistry of the surface and of the tip on the atomic scale. In practice, accuracy in the probe positioning is affected by ambient vibrations, and limits both the vertical and lateral resolution. The lateral resolution is also limited by thermal drift of the tip with respect to the sample, non-linear piezo response in the scan driver, and the finite dynamic range of the piezo driver circuit."

"Typical speeds of image acquisition are 10s for a 200x200 pixel image. However with improvements in data acquisition hardware and software, rates up to 0.1s/image have been reported. The scanning speed is ultimately limited by the shot noise in the tunneling current. However, the speed is usually limited by the lowest mechanical resonance frequency of the scanning component (tip and the piezo actuator) [49]." As STM is a scanning technique, interpretation of kinetic results need to be evaluated carefully to account for any changes in the image during the imaging time unlike the true imaging techniques discussed above. Generally speaking, the high-resolution but small-field of view data provided by STM provides an excellent complement to the lower resolution but larger field of view data of REM, LEEM and plane-view TEM.

With increasing speed of imaging, it is possible to observe rates of kinetic processes directly, and with atomic resolution using STM. The formation of domain structure [50], the motion of step edges [51] and of vacancies [52] have been observed in this way and there is potential for observing the motion of individual atoms on terraces [53]. Such real-time measurements, combined with the increasing capability for imaging at elevated temperatures, as illustrated in Figs. 6 and 7, will allow direct determination of elementary steps in kinetic processes as well as quantitative determination of the associated rate constants. The application of STM in studies of epitaxial growth in the static mode has been amply demonstrated [54,55]. Shadowing by the tip will, however, present challenges in experimental design for *in-situ* studies of growth.

### II.b Spatially Resolved Spectroscopy

A continuing important scientific problem is the correlation between structure and function on surfaces. Thus it is very important to identify how physical structures observed on surfaces influence properties such as reactivity, band bending, magnetism, conductivity and many others. A very powerful development in this area of research is

the increasing capability to measure such properties directly with spatial resolution comparable to the resolution with which structural features can be observed. Such capabilities are now realistically available in variants of Scanning Electron Microscopy which allow chemical analysis via detection of Auger and selected secondary electrons (MIDAS), as well as determination of surface magnetism by using spin-polarized detection (SEMPA). In addition PEEM provides the capabilities of spatially mapping the chemical and electronic structure by selection of specific emission lines, while spin-polarized LEEM allows a similar mapping of magnetic structure. Finally, variants of STM, scanning tunneling spectroscopy (STS), scanning micro-cathodoluminescence, and a more distant relative, near-field scanning optical microscopy (NSOM), provide the opportunity to monitor a wide range of electronic and chemical properties with atomic or near atomic resolution. Each of these techniques is described briefly below.

Microscope for Imaging, Diffraction and Analysis of Surfaces (MIDAS)[56-60]

The MIDAS facility at Arizona State University has developed outstanding capabilities in spatially resolved imaging with chemical sensitivity, as illustrated in Fig. 8. The technique employed is based on scanning transmission electron microscopy optics with through-the lens electron detection. The instrument can be used in either a transmission or a reflection mode. The scanning electron beam used has a diameter of 1 nm, compared to typical commercial SAM instruments which have a beam size of 50 nm. The resolution is also limited by inelastic delocalization and multiple scattering of back-scattered electrons. Spatial resolution of 3 nm has been demonstrated in Auger electron images by imaging boundaries between different materials on the surface. Atomic lattice resolution has been obtained in the scanning transmission mode, so that it is possible to compare transmission images (at atomic resolution) of bulk defects with chemical Auger electron images of features on the surface of a thin film. Since both the STEM detector and the Auger electron spectrometer operate simultaneously, these scanned images are in perfect registry. Other detectors supplying simultaneous spectroscopic images include the secondary electron image and the transmitted electron energy loss image.

Imaging can be performed by using the secondary energy analyzer set at one specific energy band pass to allow elemental contrast in the structural images. In this mode the rate of image formation can be 1 minute for low energy secondaries, and fifteen minutes or a little slower for higher energy excitations due to noise limitations. Imaging could also be performed in a mode in which a wide band spectrum is obtained at each

spot, allowing a complete elemental map of the surface to made. In this mode, the time for obtaining an image would depend on the spectral range sampled. For a detailed single-element Auger-electron map, a 256x256 pixel image can now be obtained in 20 minutes. The sensitivity of the instrument is such that clusters of as few as 20 silver atoms can be detected with elemental specificity.

"A technique which combines the need for high speeds, high sample temperatures and spectroscopic imaging is the scanning reflection imaging (SREM) method [61]. Here 100 keV electrons are used in the RHEED geometry, but a small sub-nanometer sized probe is formed, and a portion of the resulting microdiffraction RHEED pattern is used to form the scanned image. By stopping the probe, one obtains the RHEED pattern at a known point in the SREM image, while in addition the X-ray emission spectrum and energy loss spectrum may also be obtained from that image region. The quality of the images has recently become almost competitive with REM, whilst providing essential spectroscopic and chemical information. In principle an Auger spectrometer could be fitted to this arrangement, in which the resolution is about the same as REM (0.9 nm). The method has proven powerful for analyzing the sources of diffuse scattering in RHEED, since scattering from steps or phonons can be distinguished by stopping the probe at surface steps and observing the micro-RHEED pattern [62]."

Scanning Electron Microscopy with Polarization Analysis [63-67].

Spatially resolved magnetic information can be obtained by analyzing the vector components of the spin polarization of electrons emitted from a magnetic material. A powerful method of doing this is to use a scanning electron microscopy coupled with polarization-sensitive detectors. "Scanning electron microscopy with polarization analysis (SEMPA) measures the secondary electron spin polarization, that is the degree of orientation of the electron magnetic moments that give rise to the magnetization in a ferromagnetic material. The polarization measured in SEMPA is proportional to the magnitude and direction of the magnetization at each point probed by the incident high resolution SEM electron beam. The magnetization image is measured simultaneously with the conventional topographic image but is independent of it. A spatial resolution of 50 nm is obtained with an SEM with a $LaB_6$ cathode; 10-20 nm resolution can be obtained with a field emission cathode. The resolution is limited by the requirement of sufficient current in the SEM incident beam to compensate the low efficiency of electron spin polarization analysis. The surface sensitivity of SEMPA, of order 1 nm, requires an

ultrahigh vacuum environment to ensure that the secondary electrons measured are from the clean ferromagnetic surface, not from a contamination layer [68]."

SEMPA has been applied to a range of systems including Fe, Co, Permalloy, TbFe magneto optic recording media, hard disc recording media, magnetic insulators with a metal overcoat, and to magnetic multilayers. It has demonstrable future applicability in both fundamental studies of magnetism and in practical applications such as high-density magnetic storage devices. Implementation of high current field emission sources in the SEM will allow the present imaging time of 1-1000s per image to be decreased.

Photo-electron Emission Microscopy [38-43]

As discussed in the section on real-time in-situ measurements, photo-electrons can be collected and focused to provide an image of the surface variations in work function or composition. If the photo-electrons are not energy analyzed, the spatial resolution of this technique is limited by chromatic aberrations, and specific information as to the chemical species giving rise to the image contrast is not available. Using a threshold emission technique, in which excitation of only a narrow energy band near the work function edge is allowed, permits the spatial resolution to be increased to below 10 nm. However, to obtain spatially resolved spectroscopic information, it is necessary to add an energy filter to the imaging optics. The corresponding decrease in signal intensity has been compensated by using synchrotron radiation sources, which provide the additional benefit of a tunable photon energy, and extension of the spectral range into the X-ray region. In the X-ray region, contrast mechanisms include both core-level contrast and contrast due to extended absorption fine structure. Energy analysis can be performed with multilayer mirror optics, zone-plate optics, or with electron lenses. Resolution to 50 nm has been demonstrated for still images, and improvements in resolution to 3nm are expected at the Advanced Light Source (ALS).

Variation in this technique include the use of circularly polarized X-rays to image magnetic domains via magnetic chromatic X-ray dichroism, and the use of a scanning technique, scanning photoemission electron microscopy which has demonstrated resolution of 1 μm using threshold energies, and of 100 nm using soft X-ray core levels.

Scanned Probe Techniques

As noted above, contrast in scanning tunneling microscopy is dependent on the local density of states of the sample. Many workers have taken advantage of this fact to

probe the local electronic structure of the surface by measuring the variation in tunneling current as a function of the applied tunneling voltage. These I-V curves provide information about the surface electronic structure near the Fermi level, as well as helping to interpret the contrast mechanisms in the imaging. As would be expected, measuring a spectrum at each point in the image greatly slows down imaging, so that scanning tunneling spectroscopy (STS) provides basically still images [47]. There are many variants of STS which probe different electronic properties of the surface, and which have specialized applications. Two of the most interesting emerging scanned probe techniques provide information about the optical properties of surfaces. These are scanning micro-cathodoluminescence [69-73] and near-field scanning optical microscopy [74,75].

In micro-cathodoluminescence, the probe is a scanned tunneling tip as in STM/STS. However, the detected signal is the number of photons emitted following carrier recombination in the sample. This is accomplished by placing a fiber optic near the scanning region and collecting the photons with into a photo-multiplier tube. Noise is removed from the signal using lock-in detection. The resolution of the technique is atomic scale in the point of electron injection by the tunneling tip, and nanoscale in the area from which the resulting photons are emitted. The limitations on resolution are similar to the STM with the additional limitation of thermal noise and PMT dark current. Typical speed of image acquisition is 10-20 minutes, and is limited by the minority carrier recombination rate, which is dependent on acceptor density. The technique has been applied to GaAs/AlGaAs multilayers and quantum wells. It has potential in the study of nanostructures such as quantum wells, wires and dots, heterostructures, and superlattices. In addition there is the potential for spectroscopic evaluation of the nanostructure luminescence.

In near-field scanning optical microscopy (NSOM) [75] the traditional wavelength limit of optical imaging is overcome. This is accomplished by replacing the sharp metal tip of STM by "a tapered fiber optic tip coated by angle evaporation of aluminum, leaving an aperture of approximately 20-80 nm at the center of the tip. In transmission when a laser is coupled to the free end of the fiber, the field propagates in the fiber until the tapered tip becomes roughly the size of the wavelength of the light. At this point the field becomes evanescent and some amount of it couples through the aperture. The evanescent field gives rise to rapidly varying electric fields of high intensity. If a sample is brought close to the tip, there is a strong interaction of the light

with a volume near the aperture. If the probe is scanned across the sample, an optical image will be formed. The probe can similarly be used to collect light from the sample under far-field illumination. The image contrast in this technique arises as a result of spatial changes in the index of refraction of the sample. In addition, the rotation of the polarization of the light can be measured, giving rise to contrast resulting from variations in the local magnetic field in the sample. The resolution is limited by the aperture size, with typical values between 150-500Å. Resolution could be improved by lowering the size of the aperture. However, shrinking the aperture also limits the amount of light passing through the probe, limiting the signal detected. This problem could be reduced by improved coupling efficiency to the aperture. The rate of imaging is sample dependent, with the best values less than 1s per 256x256 pixel image. The rate is limited by the number of photons reaching the detector. The instrument can be operated in vacuum, air or liquid environment, and has been applied to a large range of systems including magnetic domains, biological samples, lithographic film exposure, localized spectroscopy of quantum well structures and florescence imaging. Promising future applications include high density magneto-optic data storage, local semiconductor spectroscopy, florescence imaging of biological samples, and high-resolution lithography [49]."

## III. Conclusions

The techniques described above provide the tools needed to make tremendous advances in many areas and applications of surface science. In applying these tools, which will provide fundamentally new types of information, it will be necessary to develop the appropriate analyses to take advantage of the data. The paradigm for doing this in the case of the real-time techniques is FIM [5,76,77], where careful statistical analysis of many images coupled with good theoretical support for understanding the mechanistic steps has led to fundamental advances in understanding. In addition, to take advantage of the potential for in-situ measurements, serious attention to instrumental design to allow imaging under real conditions will be needed: in this case the previous example of in-situ measurements using RHEED [78,79] will set the standards. (Many of the problems associated with surface defects and the difficulties they introduce into the interpretation of dynamical RHEED patterns are overcome in the microdiffraction RHEED technique of Cowley, Hembree, Ichikawa and others [80]. Quantitative analysis depends on the development of energy filters, such as the Omega

imaging filter.) Finally, in all of the techniques, but especially the spectroscopic techniques, continuing work on understanding the contrast mechanisms will be needed to interpret the measurements correctly and appropriately. Important problems here concern the need for the development of rapid *ab initio* quantum mechanical computations for the low energy methods (STM, LEED *etc.)* in order to avoid dependence on atomic potentials of dubious validity, and the problem of mixed multiple elastic and inelastic scattering for the spectroscopic imaging methods. (It is not possible at present to eliminate contrast due to elastic scattering from any of the inelastic spectroscopic images).

## Acknowledgments

The support for this workshop was provided by the Office of Naval Research under grant # N00014-93-9363, and by the National Science Foundation, Division of Materials Research, under grant DMR-9303529. One of us (EDW) was supported by the NSF under grant DMR-9023453 during the preparation of this manuscript. The workshop would not have been possible without the able organizational efforts of Ms. Donna Kroening of Northwestern University. This report would not have been possible without the cooperation of the invited speakers, listed in Table I, who provided the technical information about the various techniques described.

## References


1. M. K. Miller and G. D. W. Smith, *Atom-Probe Microanalysis, Principles and Applications to Materials Problems* (Materials Research Society, Pittsburgh, 1989).

2. T. T. Tsong, *Atom-Probe Field Ion Microscopy* (Cambridge University Press, Cambridge, 1990).

3. G. Ehrlich and K. Stolt, *Annual Rev. Phys. Chem.* 31, 603 (1980).

4. T. T. Tsong, *Surf. Sci. Rep.* 8, 127 (1988).

5. G. L. Kellogg, *Phys. Rev. Lett.* 67, 216 (1991).

6. C. S. Lent, P. R. Pukite and P. I. Cohen, *J. Vacuum Sci. Technol.* A4, 1251

7. C. S. Lent and P. I. Cohen, *Phys. Rev.* B33, (1986).

8. P. I. Cohen, G. S. Petrich and P. R. Pukite, in *Kinetics of Ordering and Growth at Surfaces*, M. G. Lagally, Eds. (Plenum Press, New York, 1990).

9. M. Gajdardziska-Josifovska, M. R. McCartney and D. J. Smith, *Surf. Sci.* 287/288, 1062 (1993).

10. D. J. Smith, M. Gajdardziska-Josifovska, P. Lu, M. R. McCartney, J. Podbrdsky, P. R. Swann and J. S. Jones, *Ultramicr.* , 26 (1993).

11. J. J. Metois, S. Nitsche and J. C. Heyraud, *Ultramicr.* 27, 349 (1989).

12. N. Osakabe, Y. Tanishiro, K. Yagi and G. Honjo, *Surf. Sci.* 97, 393 (1980).

13. N. Osakabe, Y. Tanishiro and K. Yagi, *Surf. Sci.* 109, 353 (1981).

14. M. Shima, Y. Tanishiro, K. Kobayashi and K. Yagi, *J. Cryst. Gr.* 115, 359 (1991).

15. H. Yamaguchi, Y. Tanishiro and K. Yagi, *Appl. Surf. Sci.* 60/61, 79 (1992).

16. C. Alfonso, J. M. Bermond, J. C. Heyraud and J. J. Metois, *Surf. Sci.* 262, 371 (1992).

17. E. Bauer, *Ultramicr.* 17, 51 (1985).

18. W. Telieps and E. Bauer, *Ultramicr.* 17, 57 (1985).

19. E. Bauer and W. Telieps, *Sc. Microsc.* Supplement 1, 99 (1987).

20. L. H. Veneklasen, *Rev. Sci. Instrum.* 63, 5513 (1992).

21. W. Telieps and E. Bauer, *Surf. Sci.* 162, 163 (1985).

22. M. Mundschau, E. Bauer, W. Telieps and W. Swiech, *Surf. Sci.* 223, 413 (1989).

23. R. M. Tromp and M. C. Reuter, *Phys. Rev. Lett.* 68, 820 (1992).

24. R. J. Phaneuf, N. C. Bartelt, E. D. Williams, W. Swiech and E. Bauer, *Phys. Rev. Lett.* 21, 2986 (1991).

25. M. Mundschau, E. Bauer, W. Telieps and W. Swiech, *Surf. Sci.* 213, 381 (1989).

26. M. Mundschau, E. Bauer, W. Telieps and W. Swiech, *J. Appl. Phys.* 65, 4747 (1989).

27. M. Mundschau, E. Bauer and W. Swiech, *J. Appl. Phys.* 65, 581 (1989).

28. J. Tersoff, A. W. Denier van der Gon and R. M. Tromp, *Phys. Rev. Lett.* 70, 1143 (1993).

29. M. S. Altman, H. Pinkvos, J. Hurst, H. Poppa, G. Marx and E. Bauer, *Mat. Res. Soc. Symp. Proc.* 232, 125 (1991).

30. K. Yagi, in *High resolution electron microscopy and associated techniques*(Oxford Press, 1988).

31. D. N. Dunn, R. Ai, T. S. Savage, J. P. Zhang and L. D. Marks, *Ultramicr.* 38, 333 (1991).

32. P. Xu, D. Dunn, J. P. Zhang and L. D. Marks, *Surface Science Letters* 285, L479 (1993).

33. F. M. Ross and J. M. Gibson, *Phys. Rev. Lett.* 68, 1782 (1992).

34. K. Yagi, A. Yamana, H. Sato, M. Shima, H. Ohse, S. Ozawa and Y. Tanishiro, *Prog. Theor. Phys.* Suppl. 106, 303 (1991).

35. G. Honjo, K. Takayanagi, K. Kobayashi and K. Yagi, *Journal of* Crys. *Growth* 42, 98 (1977).

36. D. N. Dunn, P. Xu and L. D. Marks, *J. Cryst. Gr.* 125, 543 (1992).

37. E. Bauer, M. Mundschau, W. Swiech and W. Telieps, *Ultramicr.* 31, 49 (1989).

38. W. Engel, M. E. Kordesch, H. H. Rotermund, S. Kubala and A. v. Oertzen, *Ultramicr.* 36, 164 (1991).

39. O. H. Griffith and G. F. Rempfer, *Adv. in Optical & Elect.* Microsc. 10, 270 (1987).

40. B. P. Tonner and G. R. Harp, *Rev. Sci. Instrum.*, 853 (1988).

41. H. Sato, Y. Tanishiro and K. Yagi, *Appl. Surf. Sci.* 60/61, 367 (1992).

42. B. P. Tonner, *Nucl. Inst. and* Meth. A291, 60 (1990).

43. G. Rempfer and M. S. Mauck, *Optik* 92, 3 (1992).

44. G. Ertl, *Science* 254, 1750 (1991).

45. B. Binnig and H. Rohrer, *Rev.* Mod. *Physics* 59, 615 (1987).

46. G. Binnig and H. Rohrer, *Helv. Phys. Acta* 55, 726 (1982).

47. J. A. Stroscio and W. J. Kaiser, *Scanning Tunneling* Microscopy Academic Press 1993).

48. C. J. Chen, *Introduction to Scanning Tunneling Microscopy* (Oxford University Press, New York, 1993).

49. Text provided by M.G. Lagally, 1993.

50. R. M. Feenstra and M. A. Lutz, *Surf. Sci.* 243, 151 (1991).

51. M. Giesen, J. Frohn, M. Poensgen, J. F. Wolf and H. Ibach, *J. Vacuum Sci. Technol.* A10, 2597 (1992).

52. N. Kitamura and M. B. Webb, *Bull. Am. Phys. Soc.* 38, 509 (1993).

53. E. Ganz, S. K. Theiss, I.-S. Hwang and J. Golovchenko, *Phys. Rev. Lett.* 68, 1567 (1992).

54. M. G. Lagally, Y. W. Mo, R. Kariotis, B. S. Swartzentruber and M. B. Webb, in *Kinetics of Ordering and Growth at Surfaces*, M. G. Lagally, Eds. (Plenum Press, New York, 1990).

55. P. A. Bennett, M. Copel, D. Cahill, J. Falta and R. M. Tromp, *Phys. Rev. Lett.* 69, 1224 (1992).

56. G. G. Hembree and J. A. Venables, *Ultramicr.* 47, 109 (1992).

57. G. G. Hembree, J. S. Drucker, F. C. H. Luo, M. Krishnamurthy and J. A. Venables, *Appl. Phys. Lett.* 58, 1890 (1991).

58. J. Drucker, M. Krishnamurthy and G. Hembree, *Ultramicr.* 35, 323 (1991).

59. J. Drucker and M. R. Scheinfein, *Physical Review* B 15, (1993).

60. M. R. Scheinfein and J. Drucker, *Physical Review* B 47, 4068 (1993).

61. J. Liu and J. Cowley, *Ultramicr.* 48, 381 (1993).

62. Text provided by J.C. Spence.

63. M. R. Scheinfein, J. Unguris, M. H. Kelley, D. T. Pierce and R. J. Celotta, *Rev. Sci. Instrum.* 61, 2501 (1990).

64. M. R. Scheinfein, J. Unguris, J. L. Blue, K. J. Coakley, D. T. Pierce, R. J. Celotta and P. J. Ryan, *Phys. Rev.* B43, 3395 (1991).

65. J. Unguris, M. R. Scheinfein, R. J. Celotta and D. T. Pierce, in *Chemistry and Physics of Solid Surfaces*, R. Vanselow and R. Howe, Eds. (Springer-Verlag, Germany, 1990).

66. J. Unguris, R. J. Celotta and D. T. Pierce, *Phys. Rev. Lett.* 67, 140 (1991).

67. J. Unguris, R. J. Celotta and D. T. Pierce, *Phys. Rev. Lett.* 69, 1125 (1992).

68. Text provided by D.T. Pierce.

69. J. H. Coombs, J. K. Gimzewski, B. Reihl, J. K. Sass and R. R. Schlittler, *J. Microsc.* 152, 325 (1988).

70. J. K. Gimzewski, B. Reihl, J. H. Coombs and R. R. Schlittler, *Z. Phys. B* 72, 487 (1988).

71. D. L. Abraham, A. Veider, C. Schonenberger, H. P. Meier, D. J. Arent and S. F. Alvarado, *Appl. Phys. Lett.* 56, 1564 (1990).

72. S. F. Alvarado, P. Renaud, D. L. Abraham, C. Schonenberger, D. J. Arent and H. P. Meier, *J. Vacuum Sci. Technol.* 9, 409 (1991).

73. P. Renaud and S. F. Alvarado, *Phys. Rev.* 44, 6340 (1991).

74. E. Betzig, J. K. Trautman, T. D. Harris, J. S. Weiner and R. L. Kostelak, *Science* 251, 1468 (1991).

75. E. Betzig and J. K. Trautman, *Science* 257, 189 (1992).

76. G. L. Kellogg and P. J. Feibelman, *Phys. Rev. Lett.* 64, 3143 (1990).

77. G. L. Kellogg and A. F. Voter, *Phys. Rev. Lett.* 67, 622 (1991).

78. P. R. Pukite and P. I. Cohen, *Appl. Phys. Lett.* 50, 1739 (1987).

79. P. R. Pukite and P. I. Cohen, *J. Cryst. Gr.* 81, 214 (1987).

80. H. Nakahara, M. Ichikawa and S. Stoyanov, *Ultramicr.* 48, 417 (1993).

81. G. L. Kellog, *Phys. Rev. Lett.* 70, 1631 (1993).

82. N. C. Bartelt, J. L. Goldberg, T. L. Einstein, E. D. Williams, J. C. Heyraud and J. J. Métois, *Phys. Rev.* B48, 15453 (1993).

83. A. W. Denier van der Gon and R. M. Tromp, *Phys. Rev. Lett.* 69, 3519 (1992).

84. S. Jakubith, H. H. Rotermund, W. Engel, A. v. Oertzen and G. Ertl, *Phys. Rev. Lett.* 65, 3013 (1990).

85. N. Kitamura, B. S. Swartzentruber, M. G. Lagally and M. B. Webb, *Phys. Rev.* B48, 5704 (1993).

86. K. Miki, Y. Morita, H. Tokumoto, T. Sato, M. Iwatsuki, M. Susuki and T. Fukuda, *Ultramicr.* 42-44, 851 (1992).

87. G. G. Hembree and J. A. Venables, *Ultramicr.* 47, 109 (1992).

88. J. Unguris, R. J. Celotta and D. T. Pierce, *Phys. Rev. Lett.* 69, 1125 (1992).

89. J. Spence, *Optik* 92, 57 (1992).

90. J. Spence and W. Qian, *Phys. Rev.* B45, 10271 (1992).

91. J. E. Bonevich and L. D. Marks, *Microscopy: The key research tool* March, 95 (1992).

92. N. Inoue, Y. Tanishiro and K. Yagi, *Jpn. J. Appl. Phys.* 26, L293 (1987).

93. J. E. Metois and J. C. Heyraud, *Ultramicr.* 31, 73 (1989).

94. H. H. Rotermund, S. Jakubith, S. Kubala, A. v. Oertzen and G. Ertl, *Journal of Electron Spectroscopy* 52, 811 (1990).

95. H. H. Rotermund, S. Jakubith, A. v. Oertzen and G. Ertl, *J. Chem. Phys.* 91, 4942 (1989).

96. H. H. Rotermund, G. Ertl and W. Sesselmann, *Surf. Sci.* 217, L383 (1989).

## Figure Captions

Fig. 1 Field Ion Microscopy observations of the motion of individual Pt adatoms on Pt(001) were used to determine mechanisms and activation energies for diffusion as a function of applied electric field. The mechanism of diffusion changes from exchange diffusion and hopping diffusion between field strengths of 1.25 and 1.5 V/Å. Figure provided by Dr. G. Kellogg of Sandia National Laboratories, Albuquerque, and reproduced with permission [81].

Fig. 2 The application of REM to quantitative measurement of kinetics of surface diffusion has been demonstrated by measurements of step motion on Si(111) at 900°C. The upper panel is a REM image of a stepped Si surface at 900°C. The dark lines are single atomic layer high steps. The average e step separation is 1400Å. As indicated on the superimposed axes, because of the glancing incidence of the electron beam, the dimension along the step edges is approximately 35 times the perpendicular dimension. The lower panel shows the time dependence of the position of a single point on one of the step edges in Fig. 1. The data set was extracted from recordings of the REM images at video-rates. The data were measured in the laboratory of Prof. J.J. Métois, and the figures are reproduced with permission [82].

Fig. 3 Real time observation of reversible faceting of a Si surface as observed by LEEM. The images, approximately 4 μm in diameter, are of a vicinal Si(111) surface misoriented by 4° toward the $[\bar{2}11]$ direction, as it is quenched through the (7x7)-to-(1x1) reconstructive transition. The bright regions are (7x7) reconstructed facets, which form as the steps move together into closely spaced bunches. The temperature of (a) is 851°C;, the temperature of (b)-(f) is 848°C. The time interval is 7.5 s between each of panels (a)-(d), and 37.5 s between each of panels (d)-(f). Figure provided by Dr. R.J. Phaneuf, of U. of Maryland, and reproduced with permission [24].

Fig. 4 The use of LEEM for in-situ studies of epitaxial growth is shown for deposition of Ag on Si(111) at ≈ 885 K. Panel a shows the clean surface. The approximately vertical lines are mono-layer high steps. Panels b-d show the conversion of the structure to a (3x1) overlayer with increasing Ag deposition. The initial nuclei form as needle-shaped structures along three crystallographically equivalent directions, and grow to cover the entire surface.

The arrow in panel d indicates a region where the structure is beginning to convert to a $(\sqrt{3}x\sqrt{3})R^{o}$ structure. Figure provided by Dr. R. Tromp of IBM Research Laboratories, Yorktown Heights, and reproduced with permission [83].

Fig. 5 The use of PEEM for in-situ studies of catalytic reactions is shown for the oxidation of CO on a Pt(110) surface. Kinetic instabilities lead to regions of spatio-temporal variation, in this case the growth of a spiral wave. The dark areas are regions covered with adsorbed oxygen atoms, while the bright areas are regions covered with adsorbed CO molecules. The width of each image is 0.2 mm. T= 434 K, CO pressure = $2.8x10^{-5}$ mbar, and $O_2$ pressure = $3.0x10^{-4}$ mbar. The images were taken sequentially at times t = 0, 10, 21, 39, 56, and 74 sec. Figure provided by Dr. H.H. Rotermund of the Fritz-Haber Institut, Berlin, and reproduced with permission [84].

Fig. 6 The use of STM to measure the kinetics of surface diffusion with atomic resolution has been demonstrated by measurements of step motion on Si(001) at 245°C. The upper set of panels, a-d, show four sequential $300x300Å^2$ images, each requiring only 15s for acquisition. The images show step rearrangement events occurring between images. The lower panel, shows a statistical analysis of approximately 750 sites, giving the probability of observing a given step column changing in position by an increment $\Delta h$ between sequential images. The data indicate an effective activation energy of 1.4 eV for the observed four-atom-unit event. Data taken by N. Kitamura and figures provided by Prof. M.G. Lagally of University of Wisconsin, Madison, and reproduced with permission [85].

Fig. 7 Real time observation of phase coexistence at the temperature of the first-order reconstructive transition of Si(111), as measured by STM. The 49x40 $nm^2$ image was measured at 1140K. Domains of 7x7 reconstruction nucleating at a step edge (near the right side) are clearly shown. The left-hand side is higher than the right-hand side. The schematic below illustrates the locations of the 7x7 unit cells observed in the image. Figure provided by Dr. K. Miki of NTT laboratories, and reproduced with permission [86].

Fig. 8 Energy selected secondary electron images of Ag islands grown on a Si substrate reveal 7 nm resolution using the 20%-80% edge resolution criterion. The upper two panels are energy selected secondary electron images, the Ag MNN Auger electron intensity map derived from those images and biased secondary electron image are shown in the lower two panels. Beam current 1.5 nA, 20 min. acquisition time for energy selected images; 0.3 nA, 1 min. for b-SEI. Figure provided by Dr. G.G. Hembree of Arizona State University, and reproduced with permission [87].

Fig. 9 SEMPA image of a the magnetization in an Fe layer covering a varying thickness Cr film (wedge) grown on a Fe(100) single-crystal whisker substrate. White regions correspond to magnetization to the right, and black regions to magnetization to the left. The short period oscillation is due to a transition between ferromagnetic and antiferromagnetic exchange as the intervening Cr film thickness changes by units of two layers. The arrows mark the Cr interlayer thickness, in atomic layers, where phase slips in the magnetization oscillations occur due to the incommensurability of the Cr spin-density wave. Figure reproduced with permission [88].

Table I: List of invited speakers at the Workshop on New and Emerging Techniques for Imaging Surfaces.

| Name | Technique |
|---|---|
| P.A. Bennett<br>Arizona State University | STM |
| P.I. Cohen<br>University of Minnesota | RHEED |
| J. Murray Gibson<br>University of Illinois | Plane-View TEM |
| M.G. Lagally<br>University of Wisconsin-Madison | STM<br>scanning microcathodoluminescence |
| G.L. Kellogg<br>Sandia National Laboratories, Albuquerque | FIM |
| L.D. Marks<br>Northwestern University | Plane-View TEM |
| R.J. Phaneuf<br>University of Maryland | LEEM |
| D.T. Pierce<br>National Institute of Standards and Technology | SEMPA |
| H.H. Rotermund<br>Fritz-Haber Institut der Max-Planck-Gesellschaft | PEEM |
| J.C.H. Spence<br>Arizona State University | MIDAS |
| B. Tonner<br>University of Wisconsin-Madison | PEEM |
| J.K. Trautman<br>AT&T Bell Laboratories | NFSOM |
| R. Tromp<br>IBM-Yorktown Heights | LEEM |
| L.H. Veneklasen | LEEM |

Table II Summary of Surface Imaging Techniques, type of probe, detector, mechanism of image constrast, and resolution.

| Name | References | Probe/Detector | Image Contrast | Resolution/<br>Source of Limitations |
|---|---|---|---|---|
| Field Ion Microscopy, Atom Probe | [1-3,77] | Electric Field Ionization of Imaging Gas/ Channel Plate Ion Detector, TOF for chemical information | Variations in Local Electric Field for structure, Field-Desorption for composition | 0.2-0.3 nm/<br>Lateral Velocity of Imaging gas ions |
| Low-Energy Electron Microscopy | [17-20] | 1-100 eV electrons/ channel plate/phosphor screen detector, or screen/TV intensifier | Diffraction | 20 nm lateral, atomic vertical/ source energy spread, lens aberrations, diffraction limit, surface roughnes |
| Low-Voltage Point Projection Microscopy | [89,90] | 100 V electrons/ channel plate detector | electron scattering | 1 nm<br>unknown |

| Name | References | Probe/Detector | Image Contrast | Resolution/ Source of Limitations |
|---|---|---|---|---|
| Microscope for Diffraction, Imaging and Analysis of Surfaces (MIDAS) | [56-60] | 20-100 kV electrons/ Low-energy electron analyzer, magnetic sector high-energy electron analyzer, annular dark-field electron scintillator, PMT secondary electron detector | Diffraction/Phase contrast (primary electrons) Chemical (Auger Electrons) Work function (Secondary Electrons) | Near atomic (0.5-1 nm) tip vibration, lens aberrations, DQE/Collection efficiency |
| Near-Field Scanning Optical Microscopy | [74,75] | Photon/Solid state detection of photons | absorption, reflection, luminescence, polarization rotation, etc. | ≤20 nm/ confinement of the EM field within the Aluminum aperture |
| Photoemission Electron Microscopy (PEEM) | [38-43] | ≥ 5 eV photons Phosphor screen with channel plate | Work Function differences Photoemission from discrete electronic levels | 10 nm with threshold emission 0.2 μm without energy analyzer, video rates 50 nm demonstrated with energy analyzer, 3 nm expected |

| Name | References | Probe/Detector | Image Contrast | Resolution/ Source of Limitations |
|---|---|---|---|---|
| Plane-view UHV TEM | [30,35,91] | electron/parallel or serial detection of electrons, x-rays or loss electrons | Diffraction/Phase contrast/structure | <0.2 nm still<br>1000Å demonstrated at video rate<br>30Å predicted at video rate |
| Reflection Electron Microscopy | [12,92,93] | 100 kV electrons/ channel plate/phosphor screen | Diffraction | 10Å lateral still images<br>100Å lateral at video rates<br>3Å resolution vertical |
| Reflection High-Energy Electron Diffraction (RHEED) | [6-8,80] | 10-100 keV electrons phospor or YAG screen or Faraday | Diffraction, Refraction | coherent scattering over 1 μm |
| Scanning Electron Microscopy with Polarization Analysis (SEMPA) | [63-67] | Electron/Electron Spin Polarization Measurement | Magnetic | 50 nm, $LaB_6$ cathode<br>10 nm, Field Emission cathode/<br>Incident electron beam diameter at lowest usable beam current |

| Name | References | Probe/Detector | Image Contrast | Resolution/ Source of Limitations |
| --- | --- | --- | --- | --- |
| Scanning Micro-cathodoluminescence | [69-73] | Tunable electron tunneling/ Fiber optic collection with PMT detection using lock-in technique | Carrier recombination rate as a function of materials and electronic structure | Atomic scale injection with nanoscale detection/ thermal noise and PMT dark current on detection, vibration and electronic noise on probe |
| Scanning Photoemission Microscopy | [94-96] | 6-95 eV photo/ photoelectrons collected by electrostatic energy analyzer | elemental, chemical, workfunction, surface potential | 0.1 μm spatial with 0.3 eV energy resolution, 1 μm spatial, using threshold energy/ flux, aberrations of optics |
| Scanning Reflection Electron Microscopy | [61] | 100 kV electrons PMT/energy filter | Crystallographic | 1 nm energy loss |
| Scanning Tunneling Microscopy | [45-47] | scanned tip probe, tunneling electrons/ tunneling current | electronic density of states | <1Å lateral <0.01Å vertical |

Table III: Summary of Surface Imaging Techniques, speed, sample conditions.

| Name | Speed of Image Acquisition/ Limitations | Sample Environment | Sample damage/ Modification |
|---|---|---|---|
| Field Ion Microscopy | Instantaneous/ Photographic or Video Recording Device | $10^{-3}$ to $10^{-5}$ torr of inert gas | High field stresses<br>Field Desorption of Adsorbates |
| Low-Energy Electron Microscopy | 0.005 to 100s/image<br>Detection DQE, shot noise, collection efficiency of the optics | UHV | possible electron beam damage for molecular species |
| Low-Voltage Point Projection Microscopy | 1 s per 1024x1024 frame | UHV | none for inorganics |
| Microscope for Diffraction, Imaging and Analysis of Surfaces (MIDAS) | video rate (STEM)<br>20 minutes/frame (Auger elemental scan)<br>Shot noise, DQE, collection efficiency of analyzer | UHV | sample dependent |
| Near-Field Scanning Optical Microscopy | Frames per second/<br>shot noise (photon flux) | vacuum, ambient, liquid | Possible photochemical degradation/ not yet observed |

| Name | Speed of Image Acquisition/ Limitations | Sample Environment | Sample damage/ Modification |
|---|---|---|---|
| Photoemission Electron Microscopy | video/phosphor screen (5 ms) | vacuum ($10^{-4}$ torr) to UHV | none |
| Plane View UHV TEM | Video rate to several minutes per frame/<br>video detector, count rates | UHV + some X-rays, pressures to a few torr have been used | yes, slow<br>knock-on, and low-energy excitations |
| Reflection Electron Microscopy | video rate | UHV | electron beam damage |
| Reflection High-Energy Electron Diffraction (RHEED) | video rates/<br>#bits, fraction of pattern | UHV reactor, in situ measurement during growth | possible electron beam/can reduce incident current |
| Scanning Electron Microscopy with Polarization Analysis (SEMPA) | 1-1000s per frame depending on pixel density and contrast/<br>Detection efficiency | UHV/low magnetic field | possible electron beam desorption of adsorbed molecules |
| Scanning Micro-cathodoluminescence | 10-20 minutes per image<br>Minority carrier recombination rate (dependent on acceptor density) | UHV | nonintrusive |

| Name | Speed of Image Acquisition/ Limitations | Sample Environment | Sample damage/ Modification |
|---|---|---|---|
| Scanning Photoemission Microscopy | seconds for threshold energies minutes to hours for X-ray/ photon flux | UHV | none observed so far |
| Scanning Reflection Electron Microscopy | video | UHV | electron beam damage |
| Scanning Tunneling Microscopy | 10s per image typical, 100x100 pixel image in 0.1s (best achieved) Mechanical resonance frequency of instrument, shot noise of tunneling current | UHV-liquid cryogenic-high temperature | some materials sensitive to tunneling current, possible tip-modification of surface due to electric field |

Table IV: Summary of Surface Imaging Techniques, applications, and future developments.

| Name | Systems to which technique has been applied | Promising future applications | Continuing/future developments |
|---|---|---|---|
| Field Ion Microscopy | Metals, semiconductors, alloys, composites, adsorbates | Surface diffusion, atom-defect interactions, cluster nucleation | Time-resolved studies with pulsed laser heating |
| In-Situ UHV TEM | Si/O, Si/Silicides, metals | MBE | improve resolution during in-situ processing<br>application to more complex systems |
| Low-Energy Electron Microscopy | Si, refractory metals, epitaxial growth | epitaxy, dislocations, step dynamics, kinetic information | Energy analyzers for Auger mapping |
| Low-Voltage Point Projection Microscopy | none | 3-d views of crystal growth modes | inexpensive |
| Microscope for Diffraction, Imaging and Analysis of Surfaces | Thin film growth studies<br>Ag/Si, Ge/Si, Fe/Cu | Correlation of nanostructure with magnetic properties of ultrathin films.<br>Surface/bulk defect studies | Near-atomic resolution with chemical specificity<br>Surface-channeling-enhanced AES |

| Name | Systems to which technique has been applied | Promising future applications | Continuing/future developments |
|---|---|---|---|
| Near-Field Scanning Optical Microscopy | Data storage devices, biological systems (fibroblasts) | Biological imaging<br>Nanoscale spectroscopy<br>lithography, metrology | Increased speed of data acquisition |
| Photoemission Electron Microscopy | Adsorbed molecules, CO, O on metals,<br>diffusion on metals | adsorbate studies, including diffusion | improved spatial and temporal resolution using UV laser or synchrotron to increase flux, and with addition of energy separators |
| Reflection Electron Microscopy | Si, metal depostion/reaction with Si<br>oxidation of Si | Kinetic processes | |
| Reflection High-Energy Electron Diffraction (RHEED) | Metals, semiconductors, insulators | epitaxy, surface structure | routine structure analysis, quantitative disorder analysis |
| Scanning Electron Microscopy with Polarization Analysis (SEMPA) | Fe, Co, Permalloy, TbFe magneto-optic recording media, hard disk recording media, magnetic insulators with metal overcoat | Magnetic imaging of high density magnetic storage devices | Implementation of high current field emission SEM with SEMPA |

| Name | Systems to which technique has been applied | Promising future applications | Continuing/future developments |
|---|---|---|---|
| Scanning Micro-cathodoluminescence | GaAs/AlGaAs superlattices and quantum wells | nanostructures, quantum structures, heterostructures and superlattices | spectroscopic evaluation of nanostructure luminescence |
| Scanning Photoemission microscopy | Fermi level pinning of GaAs(110) | metal/semiconductor interface, heterojunctions | New generation of synchrotron will provide increased flux needed to improve spatial and energy resolution |
| Scanning Reflection Electron Microscopy | Ceramics, Semiconductors | | Combination with X-Ray Microanalysis and Energy Loss Spectroscopy |
| Scanning Tunneling Microscopy | Semiconductors, metals, molecular adsorbates, in-situ electrodes, .... | epitaxy, chemical reaction, kinetics, surface modification | combination with optical probes, increased speed and range, ... |

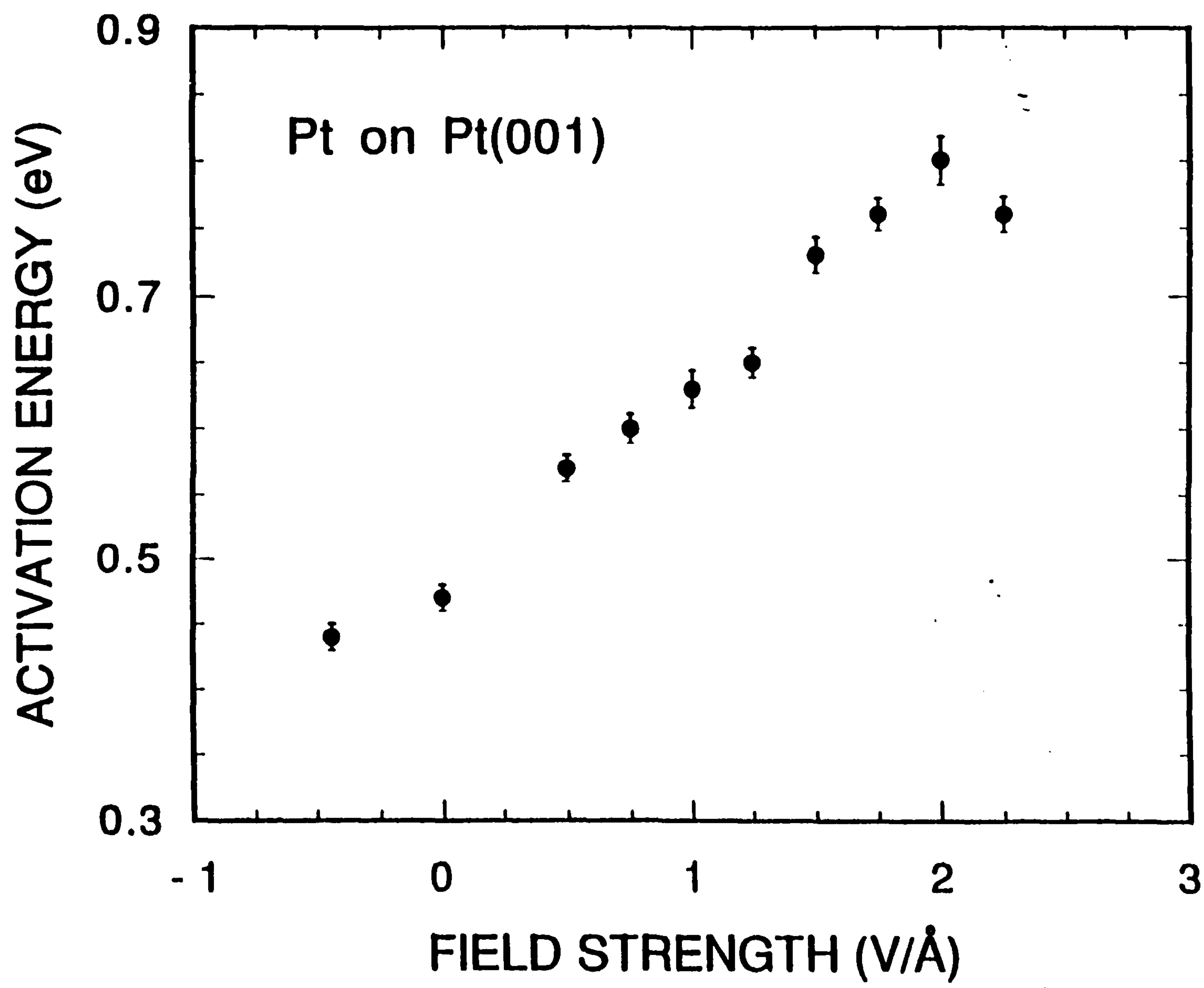


Fig. 1

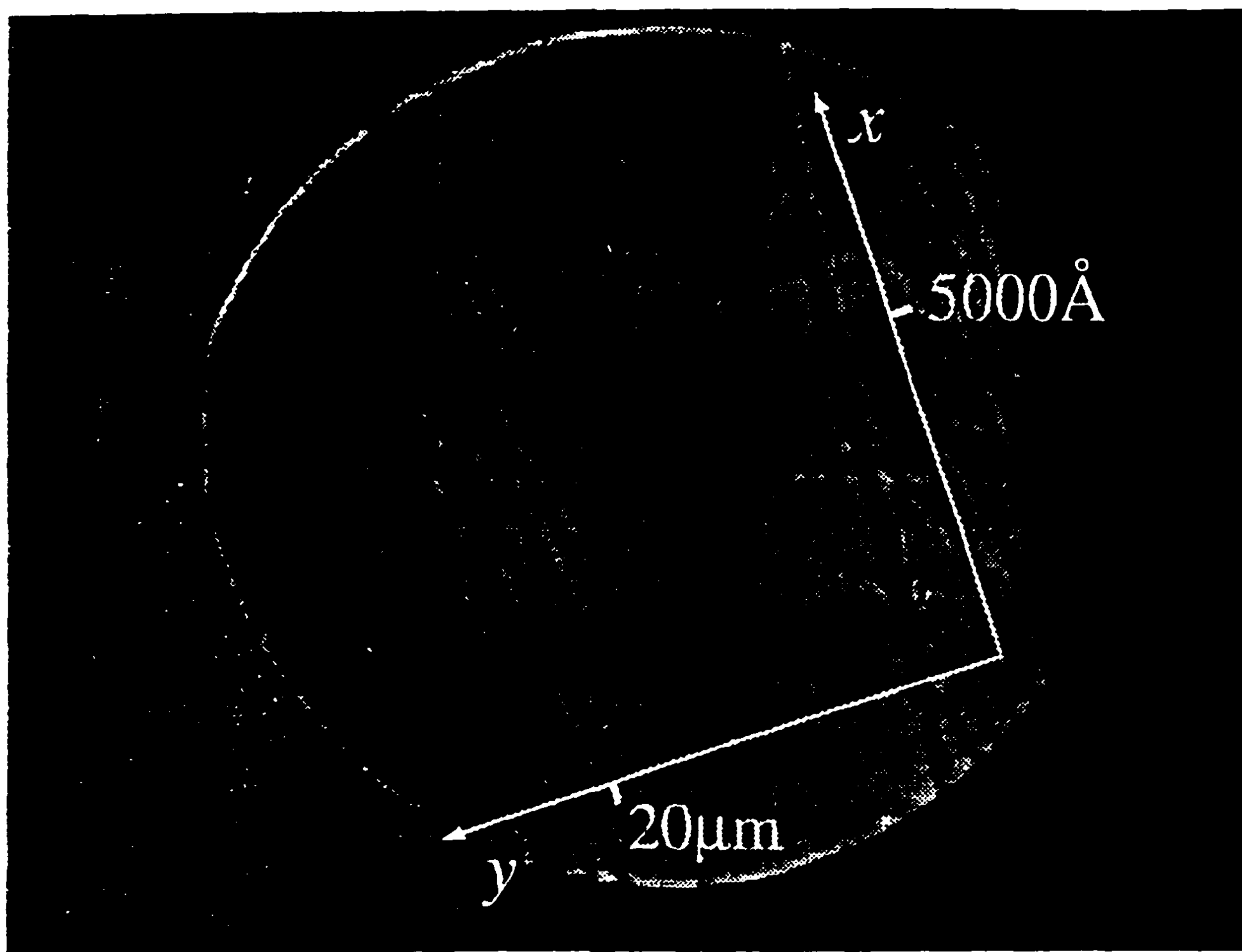
x
5000Å
20μm
y

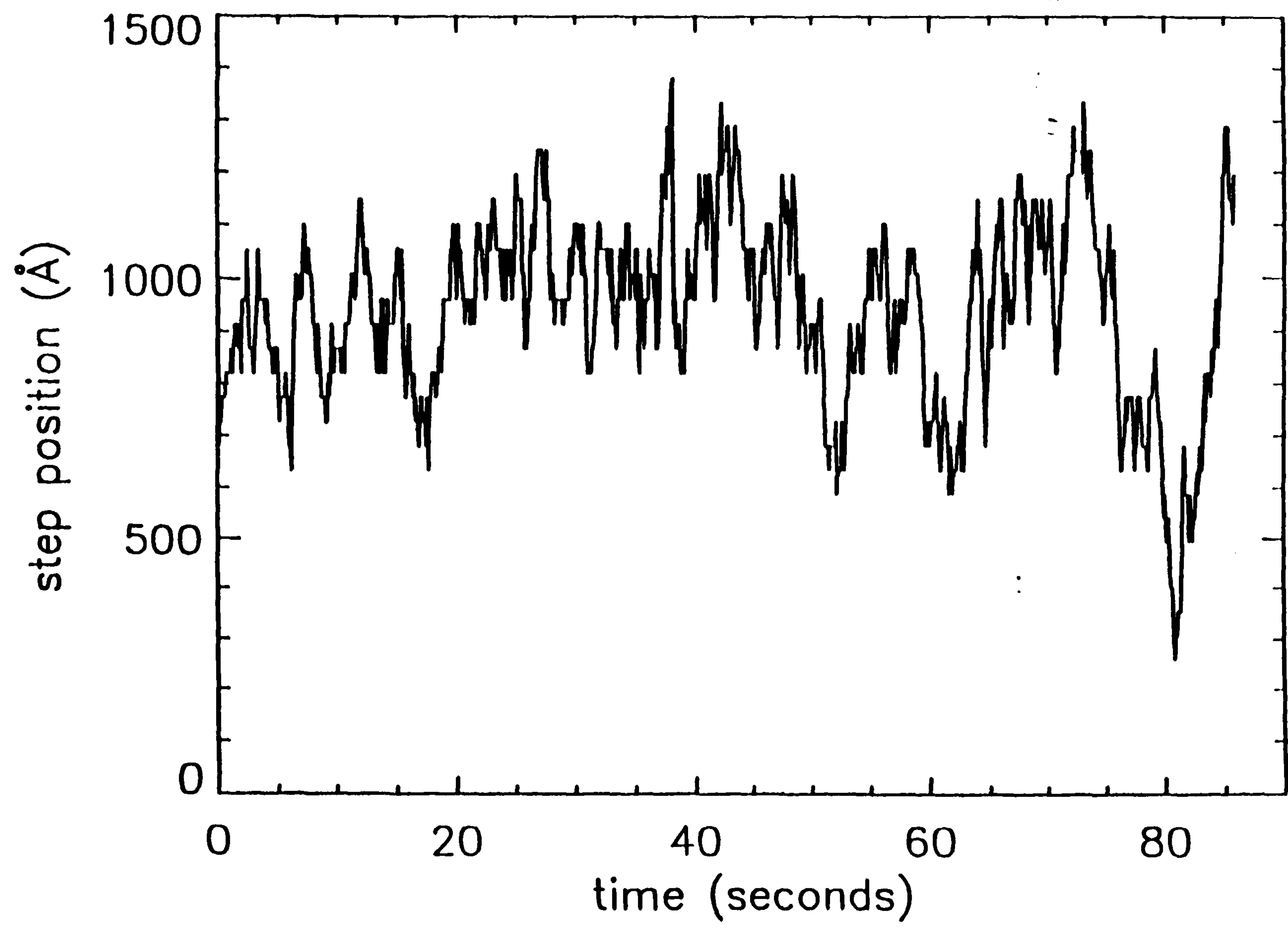
step position (Å)
1500
1000
500
0
0
20
40
60
80
time (seconds)

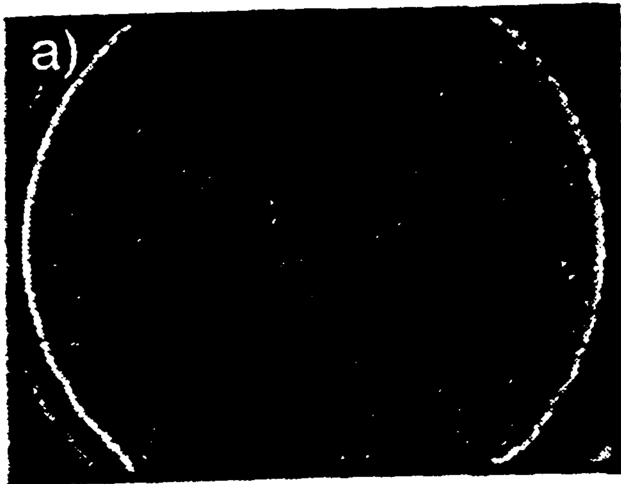
a)
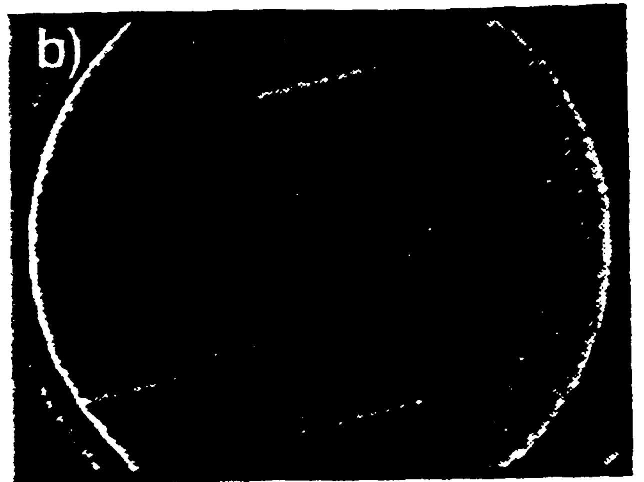
b)

c)
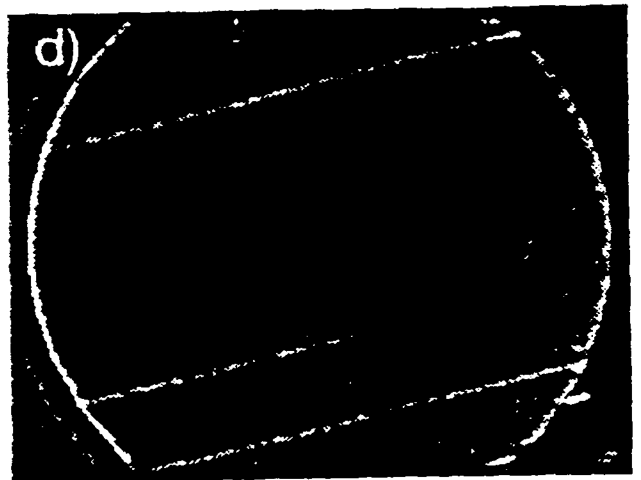
d)
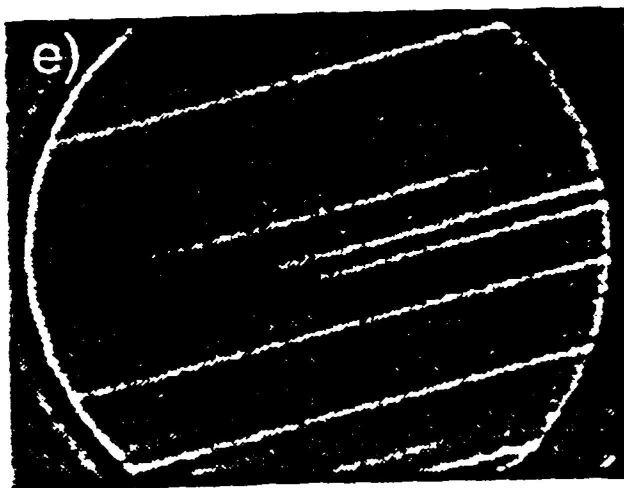
e)
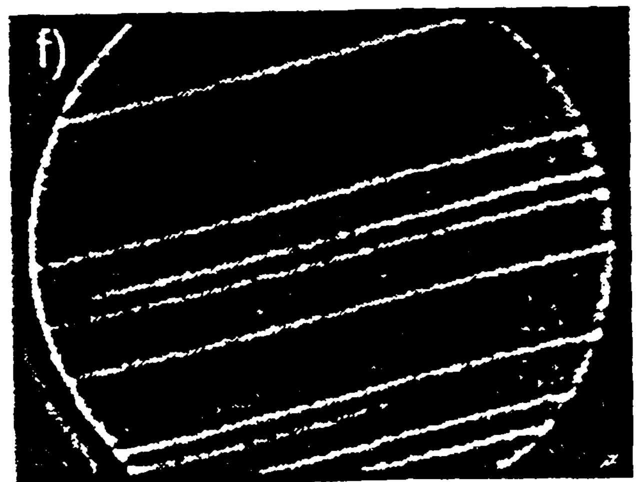
f)

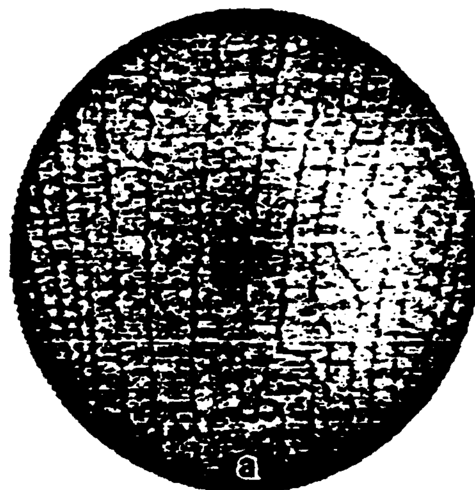
a

b

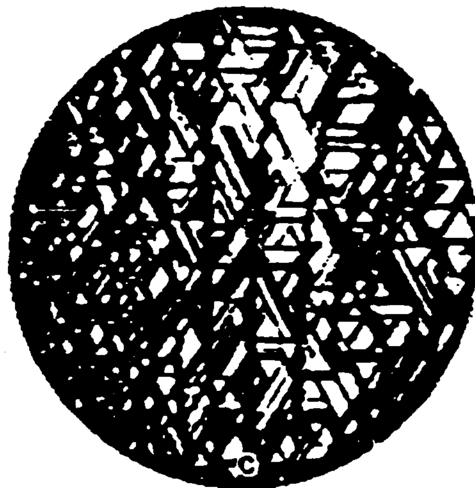
c

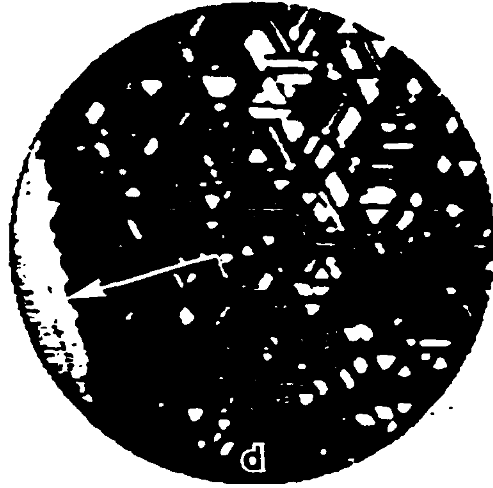
d

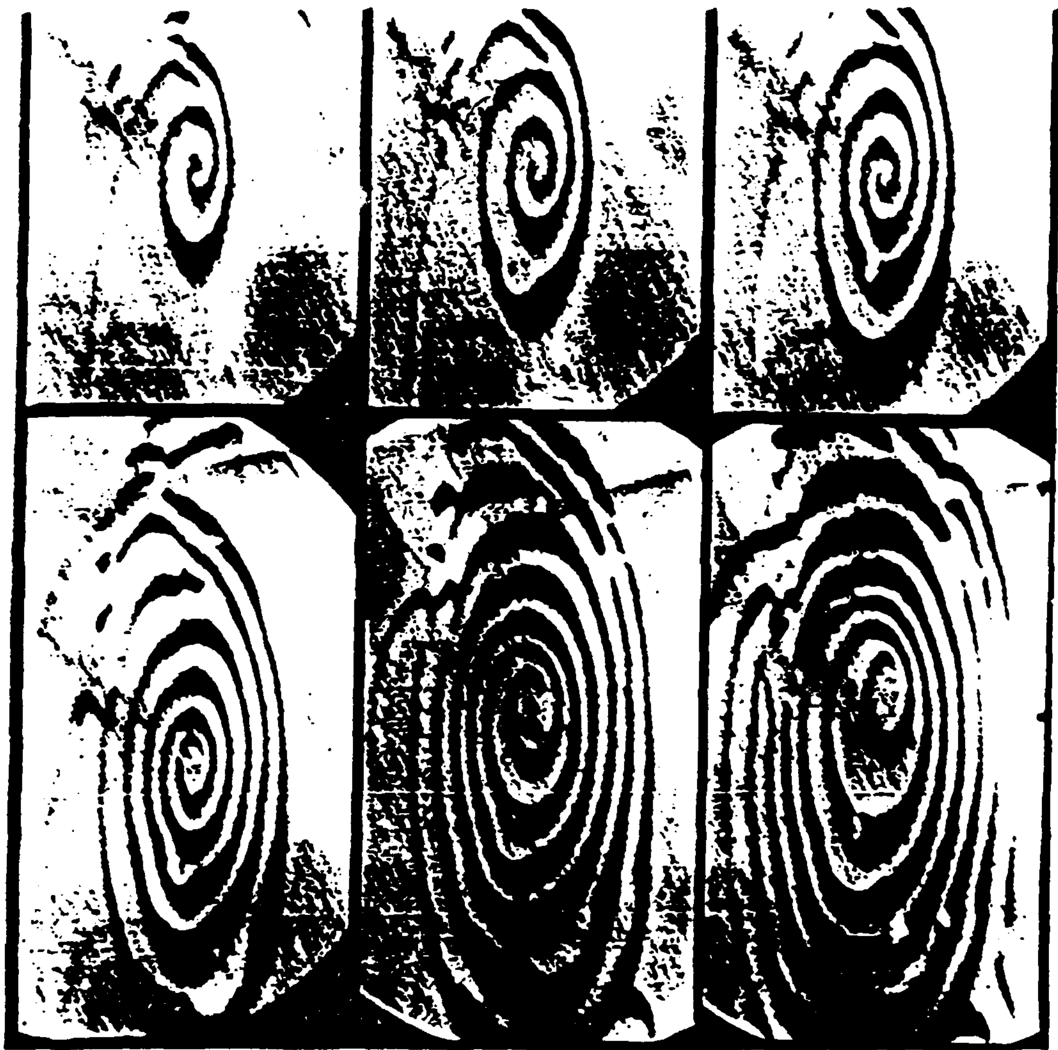

a)

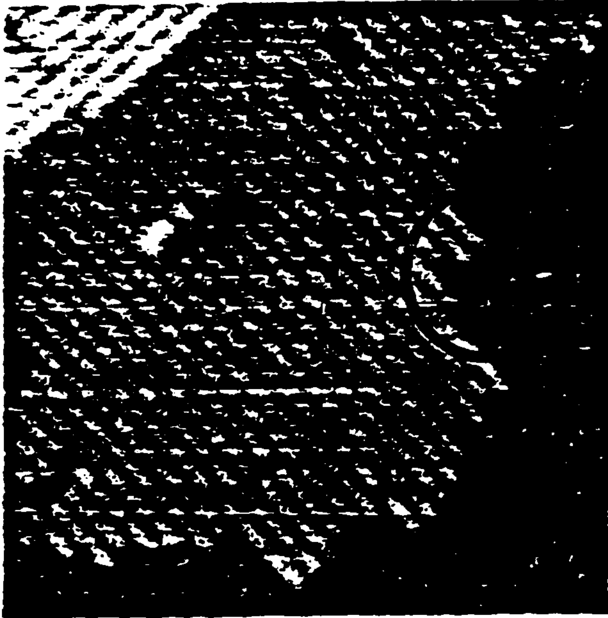

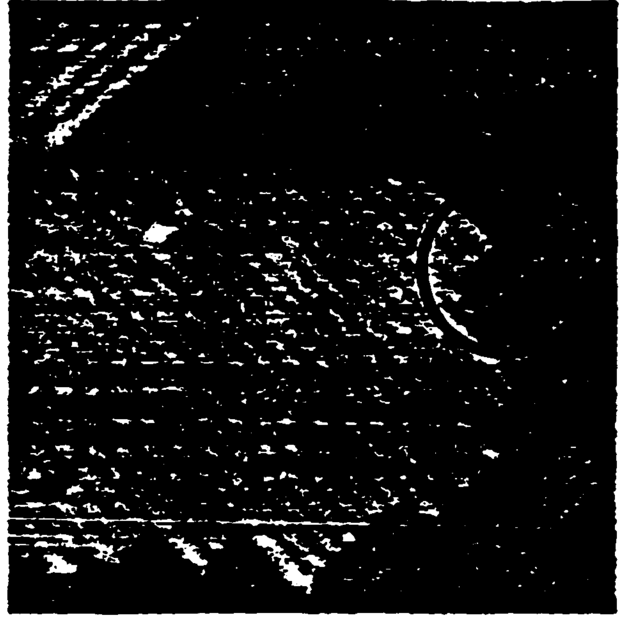

b)

c)

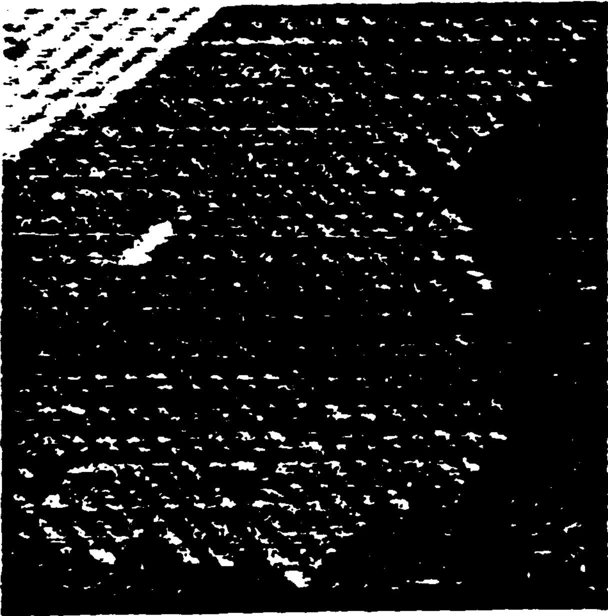

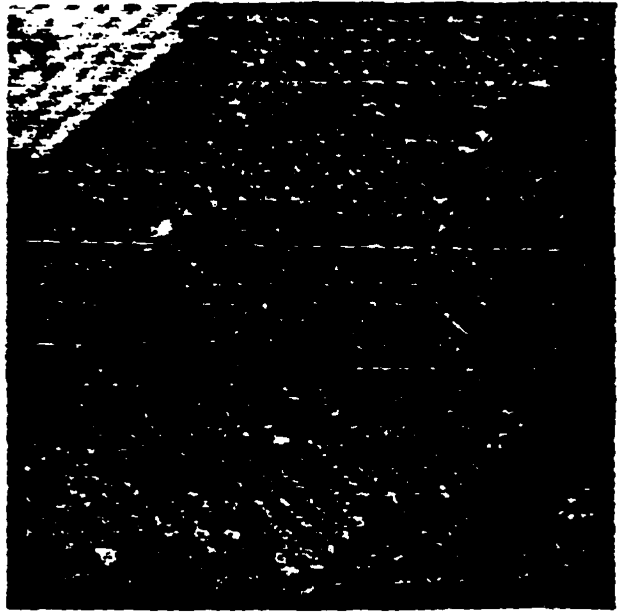

d)

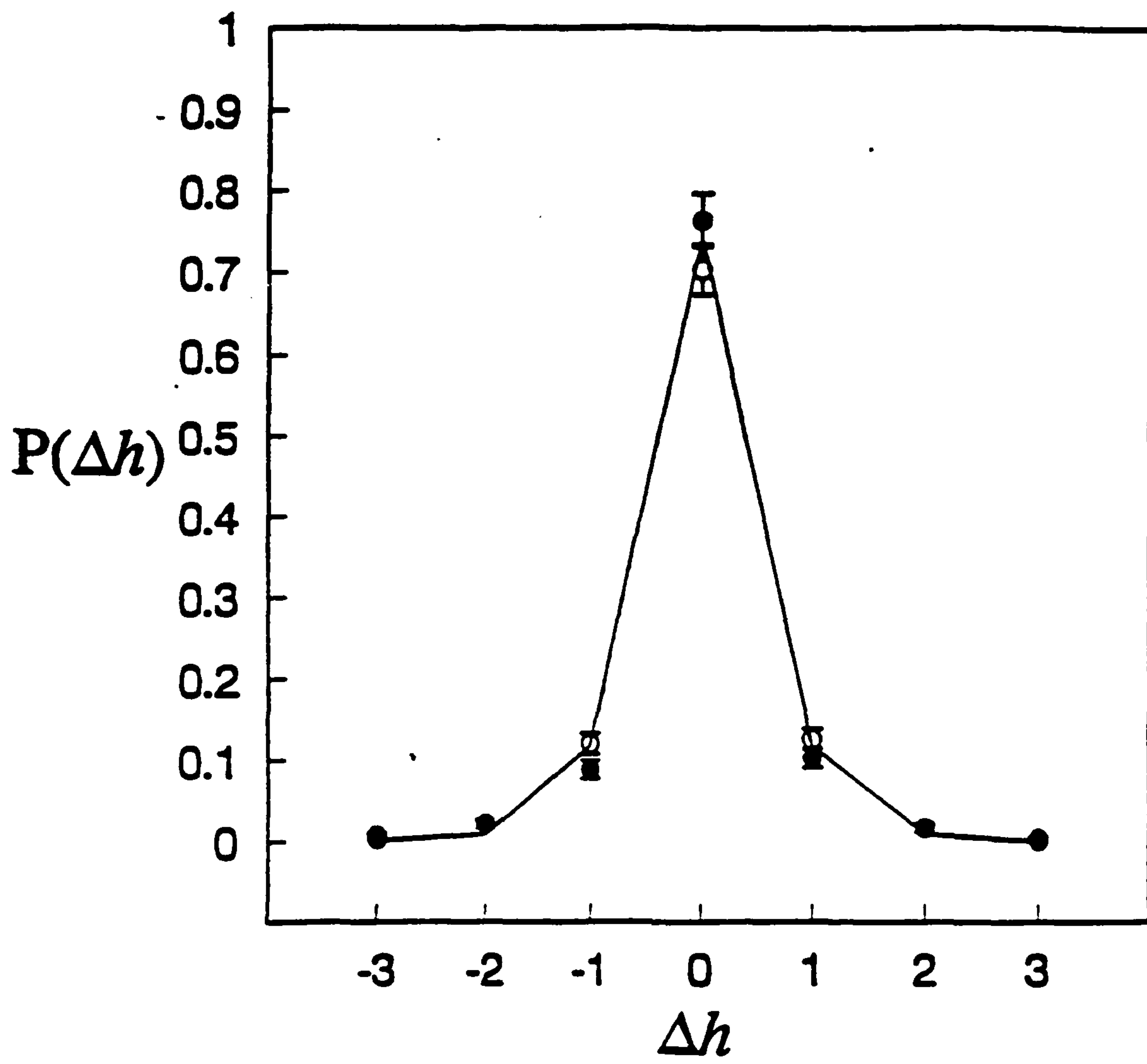
1
0.9
0.8
0.7
0.6
P(Δh)
0.5
0.4
0.3
0.2
0.1
0
-3
-2
-1
0
1
2
3
Δh

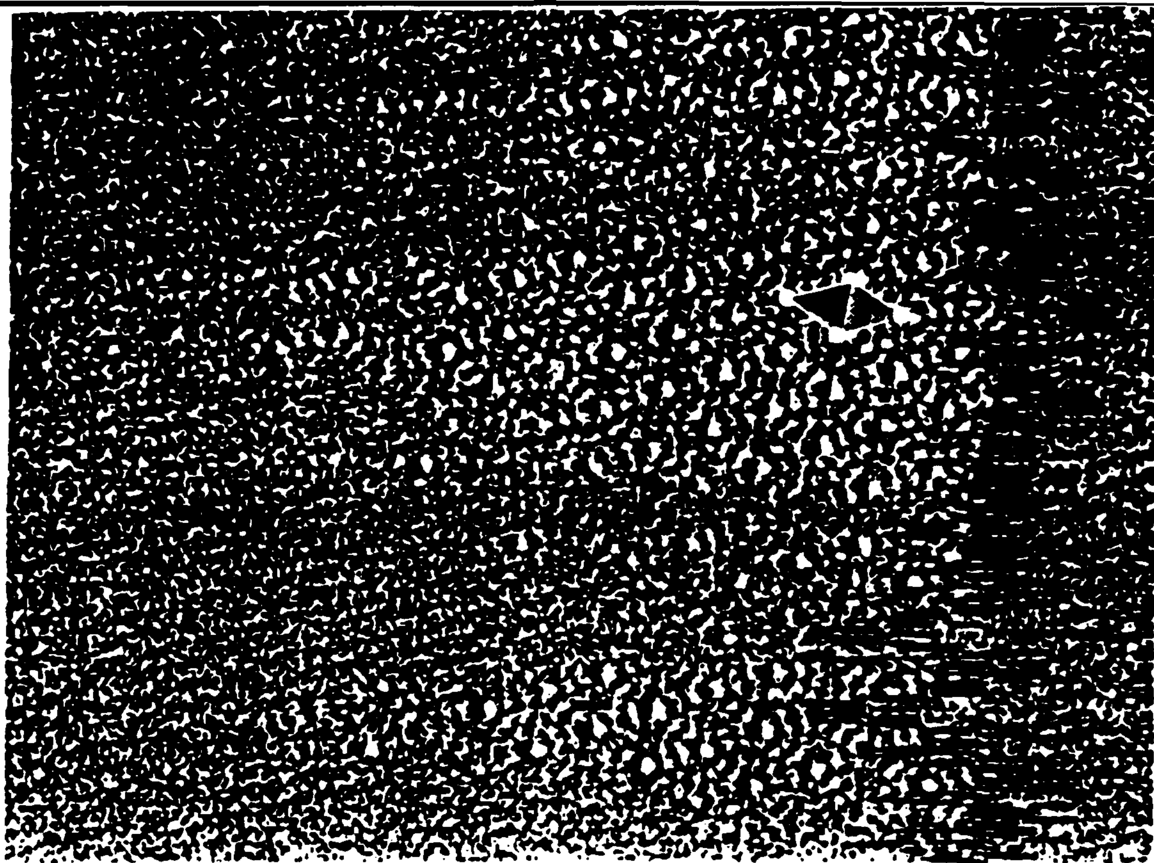

7x7 domain

1x1 phase

unfaulted triangle

faulted triangle

$[\bar{1}\bar{1}2]$-step edge

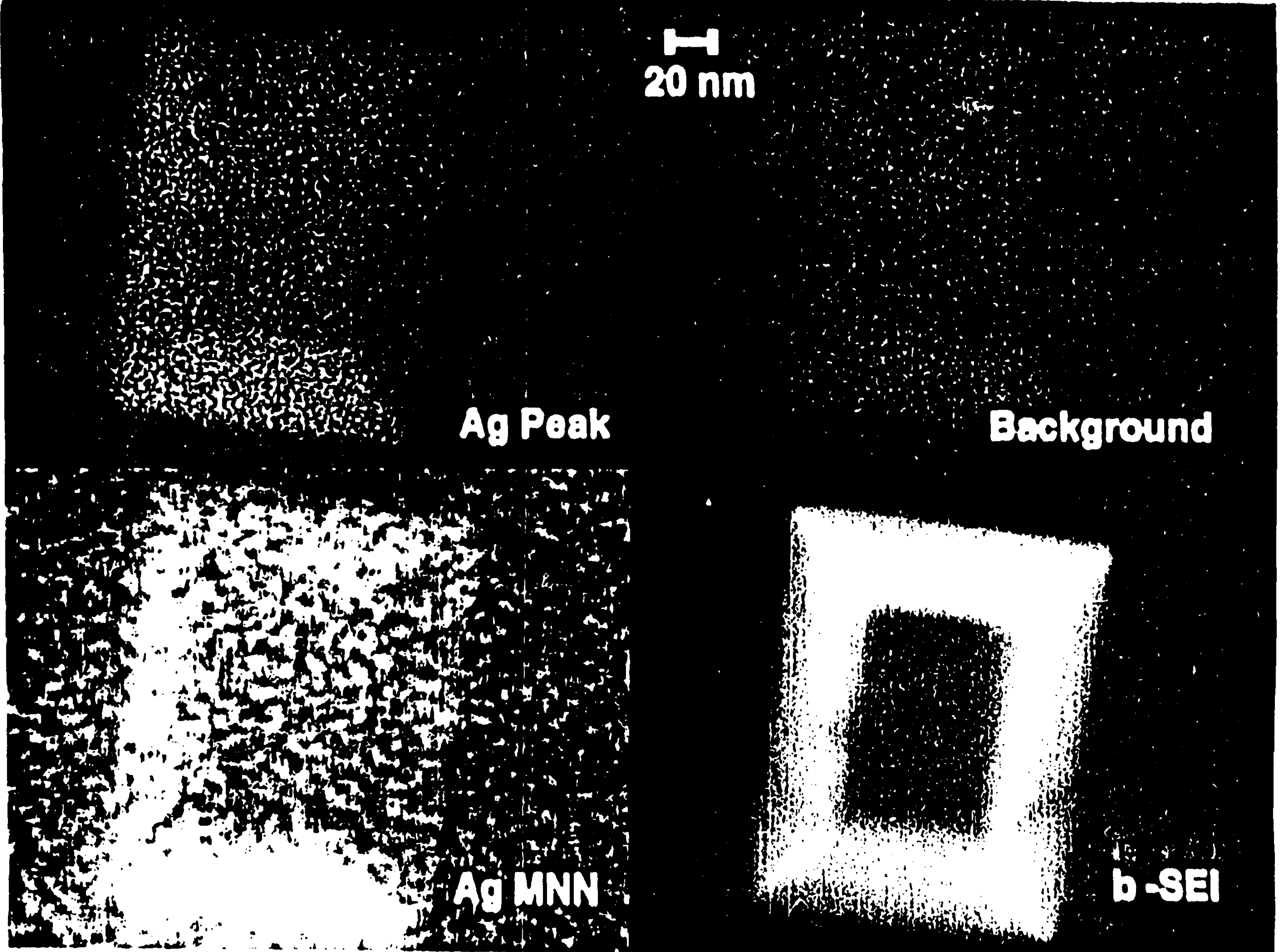
20 nm
Ag Peak
Background
Ag MNN
b -SEI

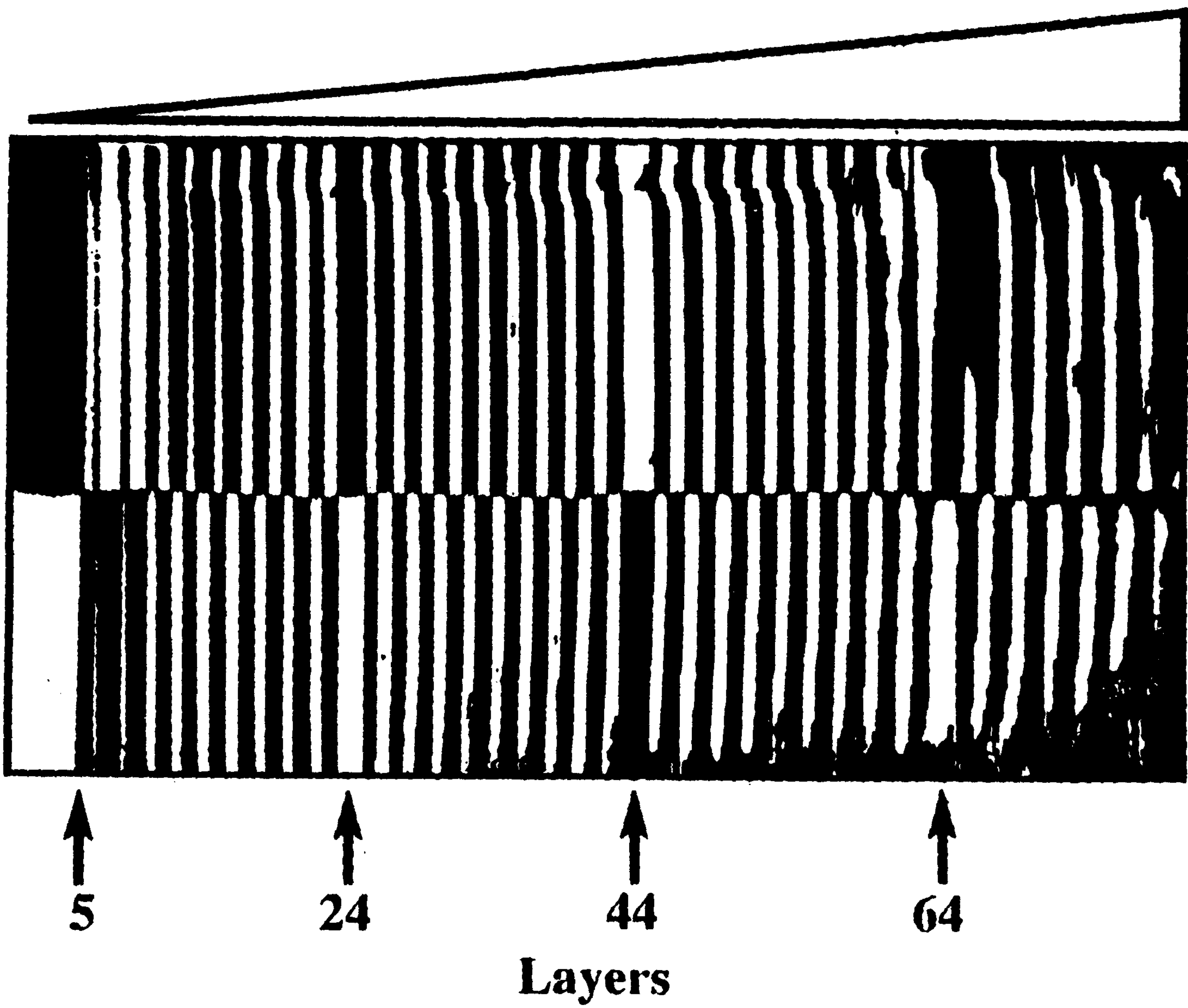


Fig. 9.

SECURITY CLASSIFICATION OF THIS PAGE

# REPORT DOCUMENTATION PAGE

| | |
|---|---|
| 1a. REPORT SECURITY CLASSIFICATION<br>Unclassified | 1b RESTRICTIVE MARKINGS<br>None |
| 2a. SECURITY CLASSIFICATION AUTHORITY | 3. DISTRIBUTION/AVAILABILITY OF REPORT |
| 2b. DECLASSIFICATION/DOWNGRADING SCHEDULE | |
| 4. PERFORMING ORGANIZATION REPORT NUMBER(S) | 5. MONITORING ORGANIZATION REPORT NUMBER(S) |
| 6a. NAME OF PERFORMING ORGANIZATION<br>Northwestern University<br>6b. OFFICE SYMBOL (If applicable) | 7a. NAME OF MONITORING ORGANIZATION |
| 6c. ADDRESS (City, State, and ZIP Code)<br>Materials Science & Engineering Dept.<br>2225 N. Campus, 2036 MLSF<br>Evanston, IL 60208 | 7b. ADDRESS (City, State, and ZIP Code) |
| 8a. NAME OF FUNDING/SPONSORING ORGANIZATION<br>Office of Naval Research<br>8b. OFFICE SYMBOL (If applicable) | 9. PROCUREMENT INSTRUMENT IDENTIFICATION NUMBER |
| 8c. ADDRESS (City, State, and ZIP Code)<br>Department of the Navy<br>Office of Naval Research, Code 1511MIC<br>800 N. Quincy St., Arlington, VA 22217-5000 | 10. SOURCE OF FUNDING NUMBERS<br>PROGRAM ELEMENT NO. / PROJECT NO. / TASK NO. / WORK UNIT ACCESSION NO. |

11. TITLE (Include Security Classification)
"New and Emerging Techniques for Imaging Surfaces" Workshop

12. PERSONAL AUTHOR(S)
Williams, Ellen D., Un. of Maryl and Marks, L. D., Northwestern University

| 13a. TYPE OF REPORT | 13b. TIME COVERED | 14. DATE OF REPORT (Year, Month, Day) | 15. PAGE COUNT |
|---|---|---|---|
| Final | FROM 1/27/93 TO 1/26/94 | 94/02/16 | 43 plus form page |

16. SUPPLEMENTARY NOTATION

Paper submitted to CRITICAL REVIEWS OF SURFACE CHEMISTRY, 1/94

| 17. COSATI CODES | | |
|---|---|---|
| FIELD | GROUP | SUB-GROUP |
| | | |
| | | |

18. SUBJECT TERMS (Continue on reverse if necessary and identify by block number)
Surface Structure, Imaging, TEM, STM, Leem, Peem, SEM, STEM.

19. ABSTRACT (Continue on reverse if necessary and identify by block number)

The development of techniques for real-time in-situ imaging of surfaces and for spatially resolved spectroscopic imaging of surfaces is reviewed. The capabilities of Field-Ion Microscopy, In-Situ Transmission Electron Microscopy, Low-Energy Electron Microscopy, Point Projection Microscopy, In-Situ Scanning Electron Microscopy, Near-Field Scanning Optical Microscopy, Photo-emission Electron Microscopy, Plane-View Transmission Electron Microscopy, Reflection Electron Microscopy, Scanning Electron Microscopy with Polarization Analysis, Scanning Micro-cathodoluminescence, and Scanning Tunneling Microscopy are summarized.

| | |
|---|---|
| 20. DISTRIBUTION/AVAILABILITY OF ABSTRACT<br>☒ UNCLASSIFIED/UNLIMITED ☐ SAME AS RPT. ☐ DTIC USERS | 21. ABSTRACT SECURITY CLASSIFICATION |
| 22a. NAME OF RESPONSIBLE INDIVIDUAL<br>L. D. Marks | 22b TELEPHONE (Include Area Code) 708-491-3996 / 22c. OFFICE SYMBOL |

DD FORM 1473, 84 MAR 83 APR edition may be used until exhausted. All other editions are obsolete

SECURITY CLASSIFICATION OF THIS PAGE

U.S. Government Printing Office: 1988—507-047